SIMPLE SIMULATION OF a-Si:H SOLAR CELLS AND THE COMPARISON WITH SPECTRAL RESPONSE

W. Kusian
Siemens AG, Corporate Research and Development, München, Germany

Keywords: semiconductors, photovoltaic applications, solar cells, description of operation, a-Si, amorphous silicon, a-Si:H, hydrogenated amorphous silicon, physical understanding, elementary models, solar cell models, solar cell simulations, PIN structures, positive-intrinsic-negative structures, PECVD, plasma enhanced chemical vapour deposition, SiH_4 silane, efficiency measurement, efficiency calculation, experimental results

Abstract: Solar cells and modules made from hydrogenated amorphous silicon (a-Si:H) have been developed for more than fifteen years. A physical understanding in simple terms of a-Si:H solar cells is made possible with the *elementary model* that uses the uniform-field approximation and neglects bulk recombination. This will be demonstrated by a qualitative discussion of dark and especially of spectral-response characteristics. Simple notions as surface recombination and flat-band voltage will be elucidated with respect to cell degradation under prolonged illumination.

Enostavna simulacija a-Si:H sončne celice in primerjava s spektralno občutljivostjo

Ključne besede: polprevodniki, aplikacije fotonapetostne, celice sončne, opis delovanja, a-Si silicij amorfni, a-Si:H silicij amorfni hidrogeniziran, razumevanje fizikalno, modeli osnovni, modeli celic sončnih, simulacije celic sončnih, PIN strukture pozitivno-notranje-negativno, PECVD nanašanje kemično s paro, izboljšano s plazmo, SiH_4 silan, merjenje izkoristka, izračun izkoristka, rezultati eksperimentalni

Povzetek: Sončne celice in moduli iz hidrogeniranega amorfnega silicija (a-Si:H) so prisotni že več kot petnajst let. Vpogled v enostavno fizikalno dogajanje znotraj a-Si:H sončnih celic nam omogočajo analitični modeli. Razviti *elementarni model* uporablja pribli'ek konstantnega električnega polja in zanemarja rekombinacije v substratu. Povedano bomo prikazali ob kvalitativni diskusiji o temni tokovnonapetostni karakteristiki in tudi karakteristiki spektralne občutljivosti. Obrazlo'ili bomo enostavna pojma, kot sta površinska rekombinacija in napetost ravnih nivojev glede na degradacijo celice pod dolgotrajno osvetlitvijo.

Introduction

Hydrogenated amorphous silicon (a-Si:H) films having electronic properties suitable for photovoltaic applications are mostly deposited by decomposition of silane (SiH_4) in a plasma enhanced chemical vapour deposition (PECVD) process. This procedure was already invented in 1969 by Chittick, Alexander and Sterling /1/, and several authors demonstrated that this material can have good electronic properties /2,3,4/. In 1975 Spear and LeComber demonstrated the doping possibility of a-Si:H that opened the way for device fabrication /5/.

Solar cells made from a-Si:H have the structure pin. For the conversion of light power into electrical power the light enters the solar cell normally through the p-layer. The photons will be absorbed within the i-layer and generate charge carriers which will then be separated by the electric field across the absorption region. Although the device quality improved very rapidly it was difficult to understand the underlying technology processes in detail and the physics of these devices. The latter can be put forward by simple or otherwise by more comprehensive solar-cell models and simulations. It is preferred here to try it with a simple analytical model first. The formulation and exemplary application of the *elementary model* will be given.

Solar Cell Operation

The understanding of a-Si:H solar cells is based on the material properties (mobilities of electrons and holes, density of localized states through the mobility gap, capture cross sections of these states) and the physics of the pin diode (drift and diffusion of mobile carriers, space charges given by the occupation of the localized states, recombination via these states). The working conditions of the solar cell are set by carrier generation under light and the external voltage. The exact simulation of the dark and light characteristics requires the numerical solution of the classical semiconductor equations (Poisson's equation, continuity equations of electrons and holes) in one dimension /6,7/.

An *exact* simulation embraces the more or less complete knowledge about the semiconductor and the pin structure. Simplifications enable *approximate* simulations or even analytical models. Simple concepts indeed helped to explain typical experiments already before the advent of exact simulations. The uniform-field concept especially has become quite useful. It assumes a spatially constant electric field right through the i-layer of a pin cell /8/. Furthermore, the i-layer alone is thought to collect photogenerated carriers, while the carriers generated within the p- and n-contact layers are immediately lost by recombination (*dead* layers). The uniform-field assumption substitutes for Poisson's equation. Thus only two of the three semiconductor equations remain active by definition, the continuity equations of electrons and holes.

The real field distribution through a pin structure becomes indeed uniform amidst the i-layer /9/. Field spikes develop towards the p-i and i-n interfaces indi-

cating partial p-i and i-n junctions. The corresponding space-charge layers near the boundaries of the i-layer depend on the high density of localized *tail states* near the valence- and conduction-band edges. The uniform-field concept now disregards the extension of the field spikes. Rather, the spikes are considered as delta functions. The associated space-charge double layers lead to potential steps through the p-i and i-n interfaces.

The uniform-field approximation considers mobile electrons and holes in the i-layer, but no trapped carriers at all. The electrons and holes remain coupled by a non-linear bulk-recombination law, after Shockley-Read-Hall for example. The electron and hole equations therefore have yet to be solved numerically. Further approximations can help to avoid that. It is most simple to neglect bulk recombination at all. The question is only whether the resulting *elementary model* /10/ has any value. Therefore the model is checked against experiments.

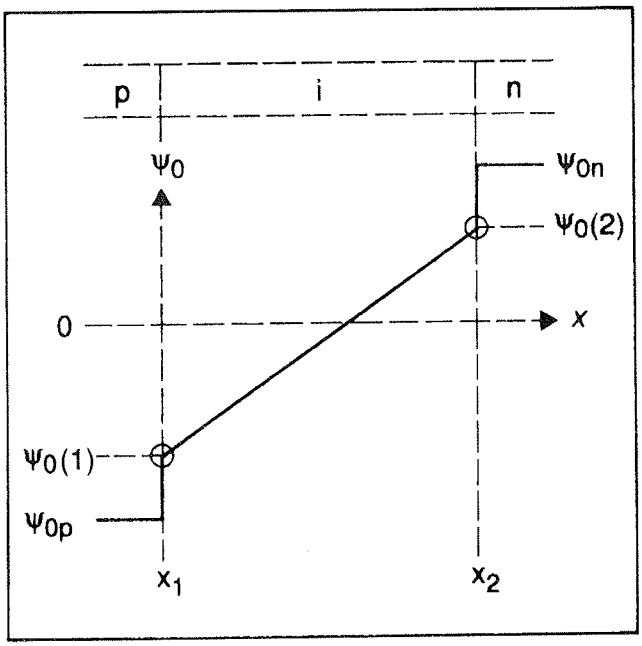

Fig. 1 *Schematic potential distribution due to the uniform-field assumption across the i-layer of an a-Si:H pin solar cell.*

The neglection of bulk recombination decouples the continuity equations of electrons and holes. The recombination then is restricted to the boundaries of the i-layer with the p- and n-layers, the p-i and i-n junctions, simply called *surfaces*. Collection of photoelectrons (photoholes) from the i-layer by the i-n (p-i) junction maintains primary photocurrents, and recombination of electrons (holes) from the i-layer with holes (electrons) from the p-(n-) layer at the p-i (i-n) junction maintains forward currents, especially secondary photocurrents. *Surface collection* and *surface recombination* are quite general notions. The elementary model (uniform-field without bulk recombination) only puts them into the foreground. So these notions alone were already helpful to interpret experimental trends /11,12/.

Elementary model

Now a formal outline of our model is presented /10,13/. The potential through a cell's pin structure according to the uniform-field assumption is sketched in Fig. 1. The electron and hole concentrations in the p- and n-layers are given by

$$n_n = n_i \exp\left(\frac{\psi_{0n}}{V_0}\right), \quad p_p = n_i \exp\left(\frac{\psi_{0p}}{V_0}\right) \tag{1}$$

with intrinsic concentration n_i, temperature voltage V_0, and "doping potentials" ψ_{0n} and ψ_{0p}. The x coordinate runs through the i-layer. The boundaries are at x_1 and x_2. The thermal equilibrium potential $\psi_0(x)$ has boundary values $\psi_0(x1)=\psi_0(1)$ and $\psi_0(x2)=\psi_0(2)$. The built-in and flat-band voltages are

$$U_B = \psi_{0n} - \psi_{0p}, \quad U_F = \psi_0(2) - \psi_0(1) \tag{2}$$

The uniform field in the i-layer without and with external voltage U is

$$E_0 = -\frac{\psi_0(2)-\psi_0(1)}{x_2-x_1} \equiv k_0 V_0, \quad E = \frac{U-U_F}{x_2-x_1} \equiv kV_0 \tag{3}$$

The field constants k_0 and k are reciprocal lengths. The potentials without and with U become

$$\psi_0(x) = \psi_0(1) - (x-x_1)E_0, \quad \psi(x) = \psi(1) - (x-x_1)E \tag{4}$$

The flat-band condition is imposed by $U=U_F$ and means $E=k=0$. The electron and hole concentrations in thermal equilibrium are

$$n_0(x) = n_i \exp\left(\frac{\psi_0(x)}{V_0}\right) = n_0(1)\exp\left[-k_0(x-x_1)\right] \tag{5}$$

$$p_0(x) = n_i \exp\left(-\frac{\psi_0(x)}{V_0}\right) = p_0(1)\exp\left[k_0(x-x_1)\right]$$

and depend on the parameters $\psi_0(1)$ and $\psi_0(2)$. The differences ψ_{0n} - $\psi_0(2)$ and $\psi_0(1)$ - ψ_{0p} are consistent with δ-like field spikes. The nonequlibrium electron and hole concentrations n and p are to be determined from the continuity equations in connection with boundary conditions. The electron and hole current densities are

$$j_n = e(D_n n' + \mu_n E n) = eD_n(n' + kn) \tag{6}$$

$$j_p = e(-D_p p' + \mu_p E p) = eD_p(-p' + kp)$$

with diffusion constants D_n and D_p, mobilities μ_n and μ_p, and $n' = dn/dx$, $p' = dp/dx$. The relations (5) let the currents (6) vanish in thermal equilibrium. The continuity equations become

$$\begin{aligned} j_n' / e &= D_n(n'' + kn') = -(g - r) \\ -j_p' / e &= D_p(p'' - kp') = -(g - r) \end{aligned} \tag{7}$$

The photocarrier generation rate $g(x)$ has to be inferred from optical modelling. The recombination rate $r(x)$ couples the relations (7) in a nonlinear fashion. These relations imply the uniformity of the total current

$$j = j_n + j_p = constant \tag{8}$$

and represent the general uniform-field equations. The elementary model puts

$$r=0 \tag{9}$$

Our boundary conditions express surface collection and recombination of excess electrons and holes, and furthermore photocarrier replenishment. The conditions are

$$\begin{aligned} j_n(1) / e &= s_n\big(n(1) - n_0(1)\big) \\ \big(j_n(2) - \beta_n j_n(1)\big) / e &= -c_n\big(n(2) - n_0(2)\big) \\ \big(j_p(1) - \beta_p j_p(2)\big) / e &= -c_p\big(p(1) - p_0(1)\big) \\ j_p(2) / e &= s_p\big(p(2) - p_0(2)\big) \end{aligned} \tag{10}$$

with boundary values $j_n(1)=j_n(x_1)$ and $j_n(2)=j_n(x_2)$, for example, to the left and right, recombination velocities s_n, s_p and collection velocities c_n, c_p. These velocities represent the two faces of a *transport velocity* /14/. The replenishment factors β_n and β_p are confined to the interval between 0 and 1. The value $\beta_n = 1$ ($\beta_n = 0$) in particular means perfect (absent) replenishment of electrons. The recombination current of electrons from the i-layer into the p-layer will be reinjected through the n-layer by virtue of the factor $\beta_n = 1$ and spares this current from being collected. A factor $\beta_n < 1$ enforces partial replenishment only. This imagined mechanism, controlled likewise via β_p for the holes, operates through the conditions (10). Replenishment hardly affects (may amplify) primary (secondary) photocurrents. The boundary value problem (7) with (9) and (10) holds for electrons and holes separately. With a function $y(x)$, representing $n(x)$ or $p(x)$, the equations (7) have the common form

$$y'' + Py' = R \tag{11}$$

with

$$P = k,\ R(x) = -g(x)/Dn$$

for the electrons and

$$P = -k,\ R(x) = -g(x)/Dp$$

for the holes. The general solution can be put together as

$$y(x) = C_1 f(x) + C_2 + \frac{1}{P}\left(\int_{x_1}^{x} R(\xi)\partial\xi - f(x) \int_{x_1}^{x} f^{-1}(\xi) R(\xi)\partial\xi \right) \tag{12}$$

with growth function $f(x)=exp(-P(x-x_1))$. The coordinate $x=x_1$ represents the left i-layer boundary, i.e. the p-i interface. The boundary conditions (10) determine the integration constants C_1 and C_2. For the flat-band case $P = 0$ the growth function becomes $f(x) = x-x_1$ and we can write

$$y(x) = C_1 f(x) + C_2 + x \int_{x_1}^{x} R(\xi)\partial\xi - \int_{x_1}^{x} \xi R(\xi)\partial\xi \tag{13}$$

The functions (12) and (13) solve the linear boundary value problem (10) and (11). The carrier concentrations in the dark and the dark characteristics stem from the inhomogeneities of the boundary conditions (10), while the right side R of the continuity equation (11) puts forth photocarriers and photocharacteristics. This remark concludes the presentation of the elementary formalism.

Dark characteristics

The comparison of the elementary model with experiments begins with the dark charcteristics. The model yields separately uniform dark currents of electrons and holes. The explicit form of the electron dark-current density is

$$j_{nD} = \frac{e n_0(1)\big(exp(U / V_0) - 1\big)}{\frac{1}{s_n} + \frac{1-\beta_n}{c_n} exp(kd) + \frac{exp(kd)-2}{D_n k}} \tag{14}$$

with $d=x_2 - x_1$ and $kd = (U-U_F)/V_0$. The flat-band case $U=U_F$ and $k=0$ yields

$$\begin{aligned} j_{nD} &= e \frac{n_0(2) - n_0(1)}{\frac{1}{s_n} + \frac{1-\beta_n}{c_n} + \frac{d}{D_n}}, \\ \frac{n_0(2)}{n_0(1)} &= \frac{p_0(1)}{p_0(2)} = exp(U_F / V_0) \end{aligned} \tag{15}$$

Similar expressions represent the hole current density, and the total dark current density becomes

$$j_D = j_{nD} + j_{pD} \tag{16}$$

as a special case of (8). Under reverse voltage $U < 0$ the current approaches the saturation value

$$j_D = -e(n_0(1)s_n + p_0(2)s_p) \quad (17)$$

or tends to the ohmic characteristic

$$j_D = \sigma_{min} E\,, \quad \sigma_{min} = e\left(\mu_n n_0(1) + \mu_p p_0(2)\right) \quad (18)$$

in case of $s_n = s_p = \infty$. Under forward voltage $U - U_F > 0$, on the other hand, and in case $c_n = c_p = \infty$ or $\beta_n = \beta_p = 1$, the dark current tends to

$$j_D = \sigma_{max} E\,, \quad \sigma_{max} = e\left(\mu_n n_0(2) + \mu_p p_0(1)\right) \quad (19)$$

It is to be understood that field $E < 0$ in (18) and $E > 0$ in (19). The current (the field) vanishes at $U = 0$ $(U = U_F)$. Current and field have opposite directions through the interval $0 < U < U_F$. Decreasing drift against diffusion lets the diode current exponentially rise through this interval. The associated quality factor is $n_Q = 1$. The field $E = 0$ at $U = U_F$ leaves a diffusion current. With $U > U_F$ the current is resistive and the characteristic bends over towards (19). Low values of the surface recombination velocities s_n and s_p retard the transition from the diode regime to the ohmic regime of the characteristic. In any case, the flat-band voltage

$$U_F = V_0 \log(\sigma_{max} / \sigma_{min}) \quad (20)$$

limits the diode regime. Fig. 2 illustrates this formal discussion. It shows forward and reverse branches of j_D after (16) assuming a *symmetric* cell (equal properties of electrons and holes, e.g. $\mu_n = \mu_p = \mu$) with the parameters of Table 1 (column A). As a check we compared with measured characteristics (see Fig. 4). The comparison indicates the following peculiarities of the elementary model: The reverse current and the factor $n_Q = 1$ are both too low (missing bulk recombination), and the characteristic becomes ohmic for $U > U_F$ (no double injection).

Table 1: Standard parameters for elementary model. Flat-band voltage U_F, potentials $\psi_0(1)$ and $\psi_0(2)$ at both sides of the i-layer in thermal equilibrium, i-layer thickness d, intrinsic carrier concentration n_i. Symmetric cells A and B with mobilities $\mu_n = \mu_p$, recombination velocities $s_n = s_p$, collection velocities $c_n = c_p$, replenishment factors $\beta_n = \beta_p$. These parameters are always used if not stated otherwise.

		A	B
U_F	[V]	0.7	0.5
$\psi_0(1)$	[V]	-0.35	-0.25
$\psi_0(2)$	[V]	0.35	0.25
d	[μm]	0.5	0.5
n_i	[1/cm^3]	10^5	10^5
μ_n, μ_p	[cm^2/Vs]	10	10
s_n, s_p	[cm/s]	10^4	10^5
c_n, c_p	[cm/s]	10^7	10^7
β_n, β_p		1	1

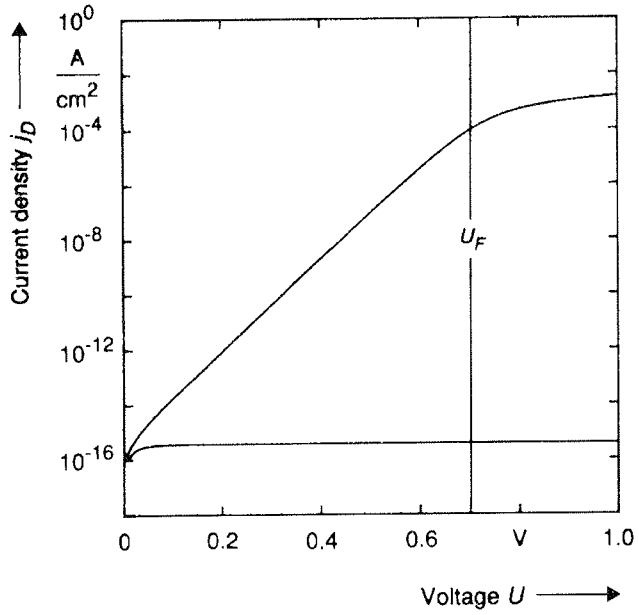

Fig. 2: Calculated dark current j_D versus voltage U, forward and reverse branches, calculated with the elementary model, parameters of table 1(column A).

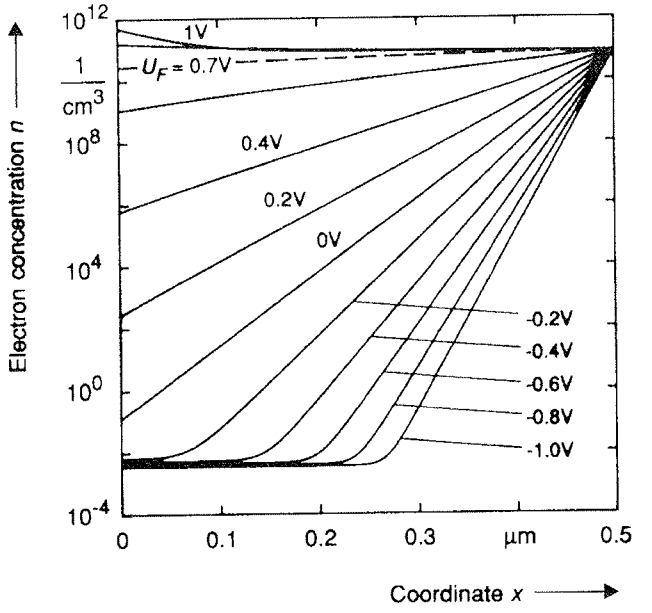

Fig. 3: Electron concentration n(x) in the dark calculated with the elementary model, parameters of table 1(column A).

The concentrations $n(x)$ of electrons and $p(x)$ of holes directly define the internal state of a pin cell. Fig. 3 shows the electron concentration associated to Fig. 2. The electrons are majority carriers in the n-layer to the right and minority carriers in the p-layer to the left. In thermal equilibrium for $U = 0$ the concentration $n(x) = n_0(x)$ follows (5). The elementary model confines itself to the I- layer. The function $n(x)$ becomes flat for $U > U_F$ and approaches the limit $n_0(x2)$ at the right side. According to Fig. 3 the electrons pile up at the left side for $U = 1$V. This behavior stems from *reverse drift* against a slowly recombining surface. Under reverse voltage $U < 0$ the electrons are pulled to the right and leave behind them a minimum concentration. The hole concentrations behave similarly as the electron concentrations.

A critical property of a-Si:H cells is *light degradation:* The efficiency comes down in the course of prolonged illumination. An anneal treatment can restore the degradation. The undegraded and degraded states are termed "A" and "B". The degradation process or the A→B transition changes the efficiency and other cell properties, including the dark currents. Fig. 4 shows as an example the measured dark characteristics of a pin cell in states A and B. Degradation increases the reverse current and the quality factor n_Q. The forward branches hence cross. The degradation process enhances bulk and surface recombination. The elementary model only offers an increase of s_n and s_p. Fig. 5 shows two modelled characteristics, one for a state A, and the other for state B. A crossing is only obtainable by a reduction of the flat-band voltage U_F for state B because $n_Q = 1$ is invariant. The observed values $n_Q > 1$ refer to bulk recombination, and the enhancement of n_Q during the degradation indicates enhancement of bulk recombination. The reduction of U_F can *simulate* enhanced bulk recombination to a certain degree. The far too low reverse currents of the modelled cell are again due to the total neglect of bulk recombination.

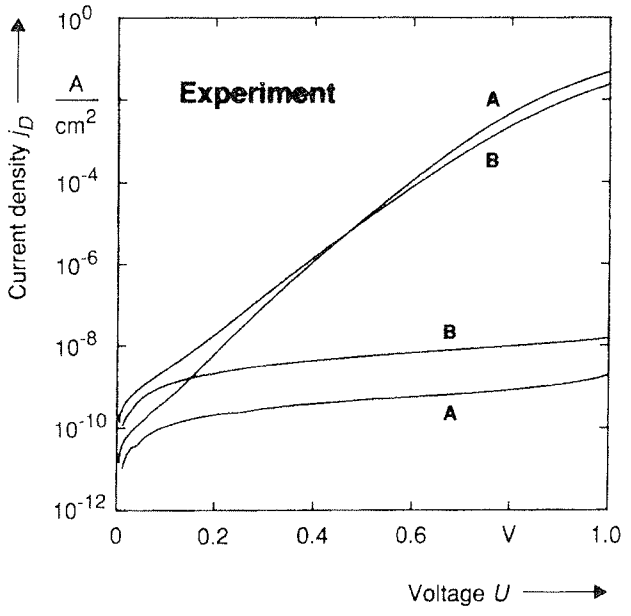

Fig. 4: Measured dark characteristics $j_D(U)$ in the undegraded state A and degraded state B.

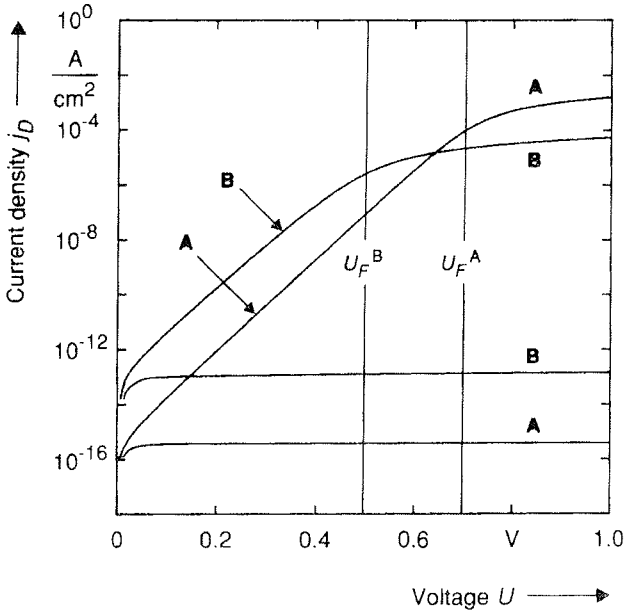

Fig. 5: Calculated characteristics $j_D(U)$ in states A and B (parameters from table 1, column A and B).

Spectral characteristics

The characteristics of a pin cell under light and in the dark are designated as $j(U)$ and $j_D(U)$. Both characteristics are measurable, and the photocharacteristic has to be derived as $j_P(U) = j(U) - j_D(U)$. A photocurrent tends under reverse voltage to a saturation current j_S, and the internal collection efficiency is by definition $q(U) = -j_P(U)/j_S$. This efficiency represents nothing else than a normalized photocurrent. It is primary (secondary) with $q < 0$ ($q > 0$). The minimum value $q = -1$ corresponds to perfect collection and $q > -1$ measures recombination losses of primary photocurrents. Values $q > 1$ are possible because the replenishment of photocarriers may amplify secondary photocurrents. The efficiency q is measurable for any illumination and may depend on light intensity. The condition $q = 0$ defines a transition voltage U_T. It generally depends on spectral composition and intensity of the respective illumination. Quite common are weak spectral illuminations, eventually in combination with a stronger background illumination. Fig. 6 shows measured $q(U)$ characteristics for a cell in the state A and a state B, found with weak spectral light of different wavelengths λ. The measurements were made with chopped signal light and without any background illumination /10/. Lock-in technique allowed to directly detect the photocurrents. Weak light should not disturb the field through a pin cell in the dark. With this condition granted the photocharacteristics probe the dark state.

The curves q-versus-U of Fig. 6 for a λ-set could be replotted as q-versus-λ curves for an U-set. A definite voltage U_P then would trace a plateau just where the A- and B-characteristics of Fig. 6 cross. The condition $q(\lambda, U_T) = 0$ defines $U_T(\lambda)$. A λ-set of $q(U)$-curves ex-

pands between the intersections $q(\lambda,0)$ with the q-axis and $U_T(\lambda)$ with the U-axis and exhibits the cross point U_P,q_P with $q_P = q(U_P)$. Degradation A→B decreases the q_P modulus and U_P, spreads the sections $q(\lambda,0)$ and $UT(\lambda)$, and decreases the section moduli. Furthermore, the "fill factor" degrades considerably, and the B-set develops two peculiarities: The "red" characteristics to the higher λ's surpass the crossing and the curved "blue" characteristic to the lowest λ shows two inflection points shortly below the crossing. Both peculiarities are in fact already present with the A-set, although in a rudimentary fashion only.

The q-sets of Fig. 6 represent an example. Its typical features pertain to any customary pin cell. The magnitudes of $q(\lambda,0)$, q_P, U_P, U_T and their degradations are quite distinguishing properties of individual cells. Is there a simple explanation for the bewildering q-phenomena? The elementary model provides it! It will be demonstrated step by step.

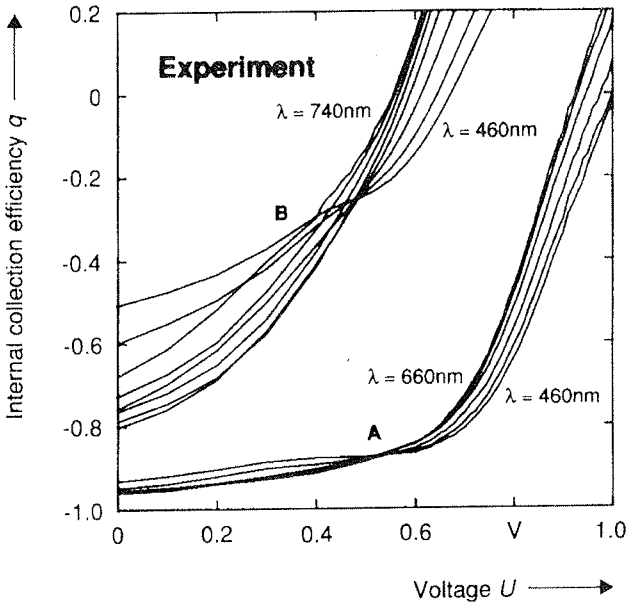

Fig. 6: Measured efficiencies q(U) at different wavelength λ of a pin diode in states A and B.

The model predicts sharp q-crossings for symmetric cells. Fig. 7 gives an example. Plotted there are two modelled q-sets designated A and B based on the parameters of Table 1. The plateau efficiency is generally given as

$$q(\lambda,U_F)=\frac{-c+(1+\beta)s}{c+(1-\beta)s+dsc/D} \qquad (21)$$

for any symmetric cell under spectral illumination /10,13/, with $s(c)$ recombination (collection) velocities, D diffusion constants and β replenishment factors of electrons and holes, and i-layer thickness d. It is only and just for $U = U_F$ that q becomes independent of the light absorption constant and λ. Thus the q-sets of Fig. 7 cross at $U_P = U_F$ through $q_P = q(U_F)$. The A→B transition was obtained by decreasing the parameters s and U_F. (The assumed degradation of U_F is exaggerated.) Let's have a short look at (21). The nominator determines the sign of $q(U_F)$. The choice $c > (1 + \beta)s$ guaranties $q(U_F) < 0$, and $s = 0$ leaves $q(U_F) = -1$. Thus a variation of s is able to shift $q(U_F)$ through the primary photocurrent regime $-1 < q < 0$. The photocurrent at $U = U_F$ is generally diffusive. Therefore $D = 0$ correctly implies $q = 0$.

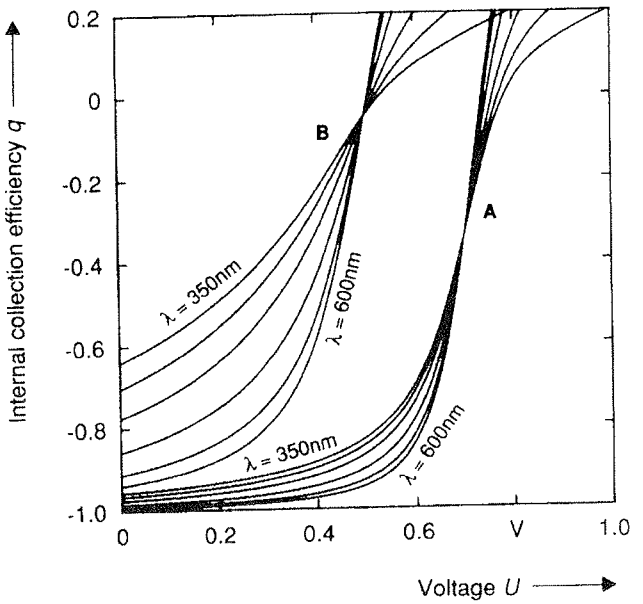

Fig. 7: Calculated efficiencies q(U) at different wavelength λ (parameters from table 1, column A and B).

The q-crossing reveals the flat-band voltage U_F. This derivation from the elementary model sticks to an ideal case, a symmetric cell. Customary pin cells are asymmetric according to $s_p > s_n$. With increasing λ the light penetrates deeper into the i-layer and just touches the back side for a certain threshold wavelength λ_t. Thus with $\lambda > \lambda_t$ the stronger back-side recombination sets in. As a consequence, the crossing is restricted to $\lambda < \lambda_t$ and the curves with $\lambda > \lambda_t$ surpass it as in Fig. 6. Just this behavior also follows from the elementary model applied to a cell /13/, and $U_P < U_F$ in addition. A measured U_P therefore indicates at best that U_F is not far away. This precaution is also necessary because the model has its own validity limits.

The unsymmetry in the junction properties of a pin diode can experimentally be pronounced by making a slightly doping of the i-layer. A doping with phosphorus ($p \nu n$) shifts the Fermi level towards the conduction band. Thus, the field spike at the p-i junction is enhanced and at the i-n junction reduced. A boron doping ($p \pi n$) acts contrarily. Theoretically, the i-layer doping influences s_n and s_p. The photocurrent behavior in such diodes strongly depends on the illumination direction. An illu-

mination through the strong field spike (i.e. low surface recombination velocity) leads to a high blue efficiency. On the other hand, an illumination through the low field spike (high surface recombination velocity) reduces the blue response and increases secondary photocurrents under forward bias. The red efficiency is in both illumination modi relatively poor.

The internal collection efficiency of *pvn* and *pπn* diodes is shown in Fig. 8 versus voltage for different wavelengths. The figure comprises both illumination modi. For illumination through the high filed spike (*pvn*) the short-circuit efficiency *q(U=0)* decreases with increasing wavelength. That means, the deeper the light penetrates into the i-layer, the stronger acts the junction with the low field spike. For illumination through the low field spike (*pπn*) *q(U=0)* increases with wavelength, because the influence of the surface recombination velocity decreases with increasing light penetration.

With the *elementary model* such characteristics are calculated and shown in Fig. 9. The parameter values are $s_n=10^3$ (10^4) cm/s and $s_p=10^4$ (10^3) cm/s for the *pvn* (*pπn*) diode. One can see, that with changing the values for s_n and s_p the overall behavior is obtained. Thus, also the slight doping of the i-layer can be described with this model.

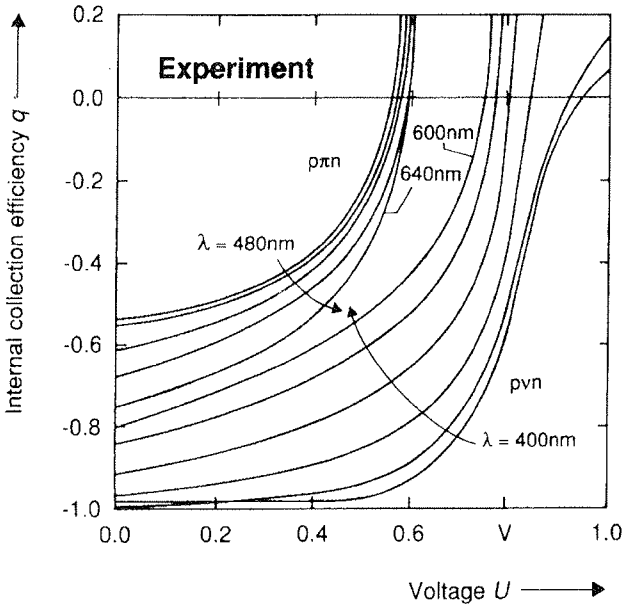

Fig. 8: Measured efficiencies q(U) for different wavelength λ of a pvn and pπn diode illuminated through the p-side.

For the following the symmetric case is regarded. An increase of s shifts any *q*-curves (of Fig. 6) upwards and broadens the short-circuit spread $\delta q = q(\lambda_2,0) - q(\lambda_1,0)$. (The relation $\lambda_2 - \lambda_1 > 0$ implies $\delta q < 0$.) This broadening effect of *s* is plausible. The penetration depth of blue (red) light is short (long) and the front-side recombination loss of electrons is high (low). The short-circuit blue efficiency will be limited by the front-side recombination velocity, whether a cell is symmetric or not. The red

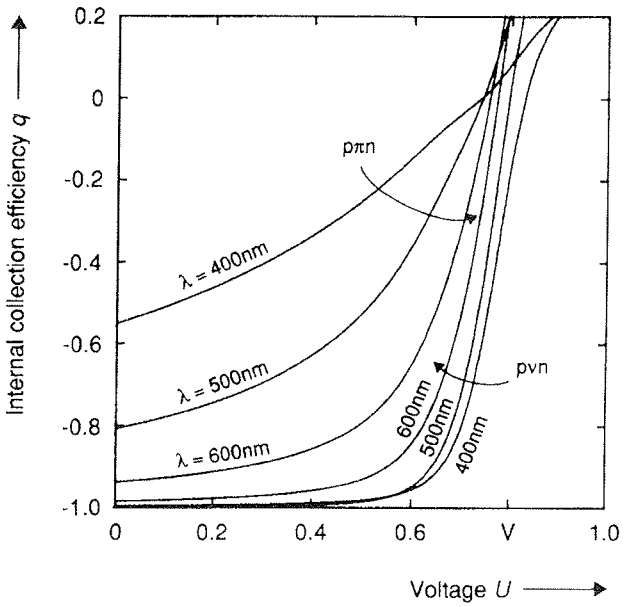

Fig. 9: Calculated efficiencies q(U) at different wavelength λ for different s_n and s_p values.

efficiency, on the other hand, will be limited by the recombination of both carriers, electrons and holes, at either side. So both velocities count. On the whole now the $q(\lambda,0)$ moduli will increase in the case $s_p > s_n$ with λ up to λ_t, because more and more electrons are collected, but with $\lambda > \lambda_t$ they again decrease, because more and more holes do recombine. This behavior is observed, e.g. with Fig. 6, and the elementary model predicts it /13/.

The measured and modelled *q*-plots of Figs. 6 and 7 are more or less similar to each other. The (exaggerated) U_F degradation indirectly simulates enhanced bulk recombination. The most conspicuous discrepancy concerns the cross or plateau efficiencies q_P. The modelled q_P are too high up (their moduli being too small). Is it possible to improve the plateau collection (to bring down the q_P-values) and leave the short-circuit spread δ_q untouched? A falling function $s_n(U)$ can do both, e.g. the one of Fig. 10 in connection with $s_p = s_n(-\infty)$. This measure transforms the *q*-sets of Fig. 7 into the sets of Fig. 11. The function $s_n(U)$ represents an arbitrary guess. It falls near a voltage U_S that is smaller than U_F, improves the collection and makes the cell asymmetric. Flat plateaus and sharp crossings do no longer exist, but a rough relation $U_P < U_F$ is to be recognized. The measured and modelled A-sets of Figs. 6 and 11 show a sharp knee near U_P. The turn-up is caused by the field reversal at $U = U_F$. Photocarriers are collected by drift and diffusion for $U < U_F$, but diffusion is dominant. Otherwise the characteristics could not be as flat. Back diffusion against drift feeds surface recombination. For $U > U_F$ collection occurs by diffusion against drift, and the surface recombination is now supported by drift. The turn-up of the characteristics indicates collection break down. The recombination is low (rising) along the flat (rising) part of the characteristics. It is the field

direction that controls surface recombination. Similar explanations apply to the B-sets. Good collection is delimited to the diode regime of the dark characteristic.

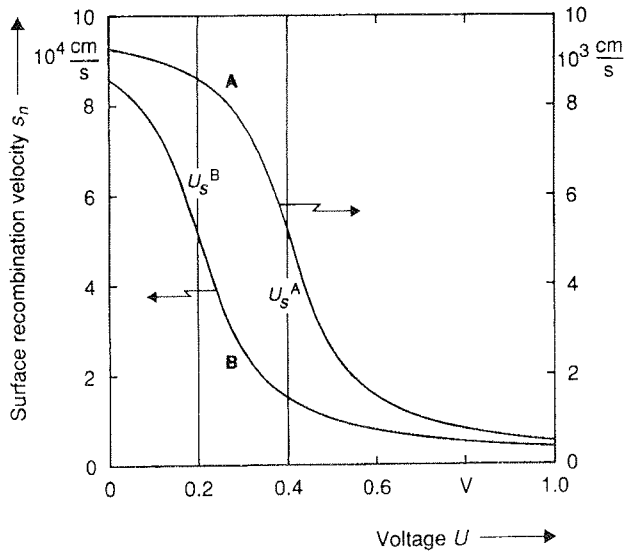

Fig. 10: Two functions $s_n(U)$ to model states A and B, U_S is the inflection voltage.

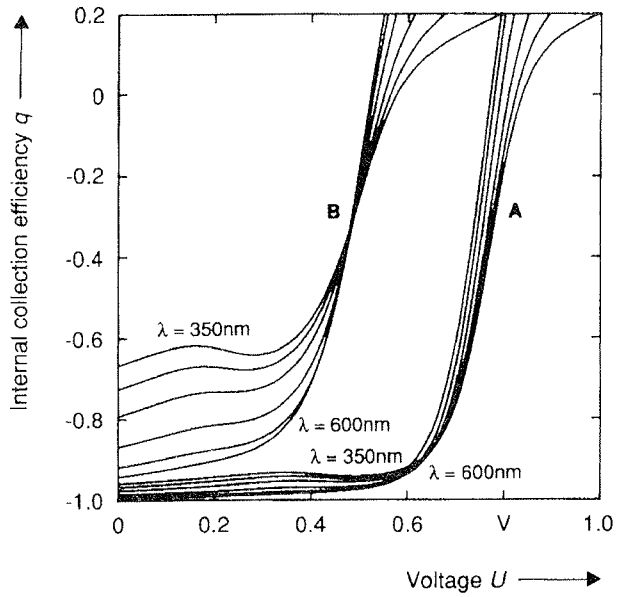

Fig. 11: Calculated efficiencies q(U) at different wavelength λ and with voltage-dependent s_n (parameters from table 1, column A and B).

The measured inflection of the B-characteristic to the shortest λ (Fig. 6) is deliberately exaggerated by our calculation (Fig. 11). The modelled "blue" characteristics even decline over a certain interval $U_S < U < U_F$ and are curved like a snake. This "blue-snake" anomaly by the way can appear also in experiments. We speak of "blue snakes" whether it comes to a slope reversal or not. The $s_n(U)$ downfall of Fig. 10 creates the blue snake of Fig. 11 and therefore simulates a real process. Customary cells have buffered p(C)-i heterojunctions. We once measured an unbuffered cell and found A- and B-sets of q without any trace of a blue snake /15/ and quite similar to Fig. 7 . Hence the blue snake is the trademark of a buffered heterojunction. Numerical simulations corroborate this conclusion /16,17/.

Discrepancies between Figs. 6 (observed) and 11 (modelled) remain: The modelled q-curves rise too steeply beyond U_F and the "fill factor" of the modelled B-set is too low. Responsible for these deficiencies are the uniform-field assumption and the neglect of bulk recombination, respectively. We have to remark that the full consideration of bulk recombination in (7) lets blue snakes appear quite naturally with constant recombination velocities s_n. So a blue snake indicates in reality a conspicuous interaction of bulk and surface recombination in the case of low-level spectral illumination!

Conclusion

The foregoing demonstrations and discussions indicate the value and the limits of the quite simple elementary model. It allows to interpret experimental characteristics and offers a first understanding of a-Si:H solar cells with respect to the most important characteristics. This comprises also the light characteristic under simulated AM1-light /18/. In order to incorporate bulk recombination a two-region model was introduced /8,19,20,21/. This two-region concept simplifies the consideration of bulk recombination. The artificial inner region boundary has to be found iteratively /19,20,21,22/, except for the simplest case (diffusion and surface recombination neglected) /8/. The neglection of bulk recombination lets the double-carrier model /22/ degenerate to our one-region elementary model /23/. The photocarrier collection occurs by drift and diffusion, and at flat-bands by diffusion alone. The distinction between minority and majority carriers becomes uncertain therefore under flat-bands, and a two-region simulation of photocharacteristics runs into serious difficulties. The flat-band situation is quite important, on the other hand. The elementary model now has no difficulty with this situation at all. Only the degenerate solution (13) has to be used. In order to fully exploit the uniform-field concept, Shockley-Hall-Read recombination rate r for example has to be considered in (7) without any further simplification. The boundary-value problem then is to be solved numerically /24/. The general uniform-field model has the potentiality to meet the experiments better than the elementary model, has also no difficulty with flat-bands, and simulates *blue snakes* without effort, as mentioned above. Simple solar cell models can in connection with experiments provide key explanations, as demonstrated here by means of our *elementary model*. The complete description of a solar cell remains the domain of *exact* simulation.

The amorphous structure and the continuously distributed density of defects has made the thorough under-

standing of a-Si:H pin solar cells very complicate. Fortunately, simple cell concepts have been proven as quite useful for the practitioner. We presented the *elementary model* as an example here. The model indentifies the significance of *flat-band voltage* and *surface recombination*, also in connection with light degradation.

References

/1/ R.C. Chittick, J.H. Alexander, H.F. Sterling, J. Electrochem. Soc. Solid State Science, Vol. 119, No. 1 (1969) 77

/2/ P.G. LeComber, W.E. Spear, Phys. Rev. Lett., Vol. 25, No. 8 (1970) 509

/3/ R.C. Chittick, Journ. of Non-Cryst. Solids 3 (1970) 255

/4/ W.E. Spear, P.G. LeComber, Journ. of Non-Cryst. Solids 8-10 (1972) 727

/5/ W.E. Spear, P.G. LeComber, Solid State Communications, Vol. 17 (1975) 1193

/6/ M. Hack and M. Shur, J. Appl. Phys. 58 (1985)997

/7/ J.L. Gray, IEEE-ED 36 (1989) 906

/8/ R.S. Crandall, J. Appl. Phys., vol.53 (1982) 3350

/9/ W. Kusian, H. Pfleiderer, AIP Conference Proceedings 234 (1991) 290

/10/ W. Kusian, H. Pfleiderer and B. Bullemer, Mat. Res. Soc. Symp. Proc., vol.118 (1988) 183

/11/ W. Kusian, H. Pfleiderer and B. Bullemer, Solar Cells, vol.22 (1987) 239

/12/ W. Kusian, H. Pfleiderer and B. Bullemer, J. Appl. Phys., vol.64 (1988) 5220

/13/ H. Pfleiderer, W. Kusian, E. Günzel and J. Grabmaier, 20th IEEE PVSC (1988) 180

/14/ M.Wolf, IEEE-ED, vol.28 (1981) 566

/15/ W. Kusian, H. Pfleiderer and W. Juergens, 9th European Photovoltaic Solar Energy Conference (1989) 52

/16/ W. Kopetzky, H. Pfleiderer and R. Schwarz, Journal of Non-Crystalline Solids, vol.137&138 (1991) 1201

/17/ H. Pfleiderer, Mat. Res. Soc. Symp. Proc. vol. 297 (1993) 791

/18/ W. Kusian, K.-D. Ufert, H. Pfleiderer, Solid State Phenomena Vols. 44-46 (1995) 823

/19/ R.S. Crandall, J.Appl.Phys., vol.54 (1983) 7176

/20/ H. Okamoto, H. Kida, S. Nonomura and Y. Hamakawa, Solar Cells, vol.8 (1983) 114

/21/ D.A. Aronov, R. Kabulov, and Yu.M. Yuabov, phys. stat. sol. (a) 118 (1990) 577

/22/ F. Irrera and F. Palma, Solid-State Electronics, vol.34 (1991) 801

/23/ W. Kusian and H. Pfleiderer, Journ. of Non-Cryst. Solids 164 - 166 (1993) 713

/24/ M. Ohnishi, T. Takahama, and Y. Kuwano, Mat. Res. Soc. Symp. Vol. 219 (1991) 421

Dr. Ing. habil. Wilhelm Kusian
Siemens AG
Corporate Research and Development
Otto-Hahn Ring 6
D-81739 München
tel.: +49 89 636 44682
fax: +49 89 636 49164
Email: wilhelm.kusian@zfe.siemens.de

Prispelo (Arrived): 12.8.1996 *Sprejeto (Accepted): 20.8.1996*